

Single cell manipulation using ferromagnetic composite microtransporters

Mahmut Selman Sakar, Edward B. Steager, Dal Hyung Kim, Min Jun Kim, George J. Pappas et al.

Citation: *Appl. Phys. Lett.* **96**, 043705 (2010); doi: 10.1063/1.3293457

View online: <http://dx.doi.org/10.1063/1.3293457>

View Table of Contents: <http://apl.aip.org/resource/1/APPLAB/v96/i4>

Published by the [American Institute of Physics](#).

Additional information on *Appl. Phys. Lett.*

Journal Homepage: <http://apl.aip.org/>

Journal Information: http://apl.aip.org/about/about_the_journal

Top downloads: http://apl.aip.org/features/most_downloaded

Information for Authors: <http://apl.aip.org/authors>

ADVERTISEMENT



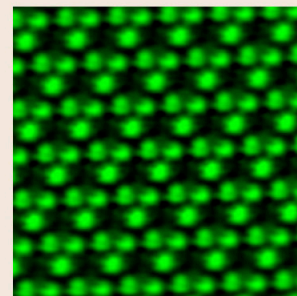
**ASYLUM
RESEARCH**
The Technology Leader in SPM/AFM

Register Now at
www.asylumresearch.com

Free AFM Webinar February 22 Register Now

“Smaller and Quieter: Ultra-High Resolution AFM Imaging”

With Jason Cleveland, AFM pioneer,
inventor and Asylum Research co-founder



Single cell manipulation using ferromagnetic composite microtransporters

Mahmut Selman Sakar,¹ Edward B. Steager,¹ Dal Hyung Kim,² Min Jun Kim,² George J. Pappas,¹ and Vijay Kumar^{1,a)}

¹GRASP Laboratory, School of Engineering and Applied Sciences, University of Pennsylvania, Philadelphia, Pennsylvania 19104, USA

²Mechanical Engineering and Mechanics, Drexel University, Philadelphia, Pennsylvania 19104, USA

(Received 5 December 2009; accepted 21 December 2009; published online 29 January 2010)

For biomedical applications, such as single cell manipulation, it is important to fabricate microstructures that can be powered and controlled wirelessly in fluidic environments. In this letter, we describe the construction and operation of truly micron-sized, biocompatible ferromagnetic microtransporters driven by external magnetic fields. Microtransporters were fabricated using a simple, single step fabrication method and can be produced in large numbers. We demonstrate that they can be navigated to manipulate single cells with micron-size precision without disturbing the local environment. © 2010 American Institute of Physics. [doi:10.1063/1.3293457]

The independent manipulation of cells and man-made objects on the micron scale in a controlled manner using autonomous microtools is one of the great challenges in microscale engineering.^{1,2} Actuation can be realized using inorganic components, and there is extensive ongoing research on developing artificially engineered micro/nanoscale structures to manipulate microcomponents.^{3–12} Previous work has also addressed different approaches to actuation and control with engineered microorganisms.^{13–18} In our previous work, we integrated swarmer cells of *Serratia marcescens* and genetically engineered *Escherichia coli* cells with negative photosensitive epoxy (SU8) microfabricated structures to construct microbiorobots. These robots were steered in a fully automated fashion using computer control, used to transport and manipulate micron-size objects, and employed as cell-based biosensors.¹⁹

This letter reports on manipulation of individual *Tetrahymena pyriformis* (*T. pyriformis*) cells using microfabricated magnetically responsive microtransporters. Specifically, iron oxide nanoparticles (magnetite, Fe_3O_4) were suspended in SU8, and microstructures with feature sizes as small as $10\ \mu\text{m}$ were fabricated with this composite ferromagnetic photoresist. Using a similar composition, magnetically actuated micromirrors have been fabricated with nickel nanospheres and SU8 photoresist.²⁰ In contrast to nickel or neodymium particles, magnetite particles are biocompatible which is an essential property needed for working with living cells. There is also a parallel line of research where magnetite particles are mixed with polydimethylsiloxane to fabricate flexible, ferromagnetic polymer structures such as millimeter-sized swimmers²¹ and tools.²²

In this letter, microstructures were fabricated in a single step that does not require subsequent lithography or etching processes. Although magnetite nanoparticles are opaque, standard lithography still works as reflection, scattering and diffraction of light from the particles assist in the proper exposure of the photoresist.²⁰ The ferromagnetic photoresist was prepared by mixing iron oxide powder (spherical, 50 nm in diameter, Alfa Aesar, IL, USA) with SU8–25 (MicroChem, MA, USA) in a glass Petri dish until it yielded a

homogenous suspension. We waited one hour before using the photoresist to eliminate entrapped air bubbles. The microstructures were fabricated on glass slides using one step photolithography. The fabrication sequence is shown in Fig. 1(a). The first spin-coating procedure was used to prepare the nontoxic water-soluble sacrificial dextran layer.²³ This layer is needed to release microstructures into the fluidic chamber without causing any structural damage. An aqueous solution of 5% (w/v) dextran 50–70 kDa was spun onto the glass slide, and baked. Next, the ferromagnetic photoresist was spin coated. The exposed substrate was postbaked and developed in propylene glycol monomethyl ether acetate. The glass slide was kept in 3% HCl (w/w) solution for 1 min to dissolve excess iron oxide particles, then washed with deionized water and dried with nitrogen air. Finally, microstructures were magnetized for 5 min using a rectangular neodymium-iron-boron (NdFeB) magnet with a surface field of 6450 Gauss (K&J Magnetics, Jamison, PA). We varied the weight ratio of the particles suspended in the photoresist

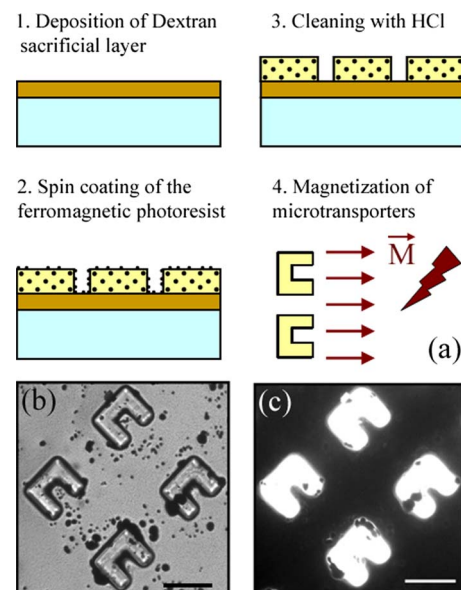


FIG. 1. (Color online) (a) Fabrication sequence for the microtransporters. Phase contrast (b) and fluorescence (c) images of $100 \times 110 \times 50\ \mu\text{m}^3$ U-shaped microtransporters. The scale bar is $100\ \mu\text{m}$.

^{a)}Electronic mail: kumar@seas.upenn.edu.

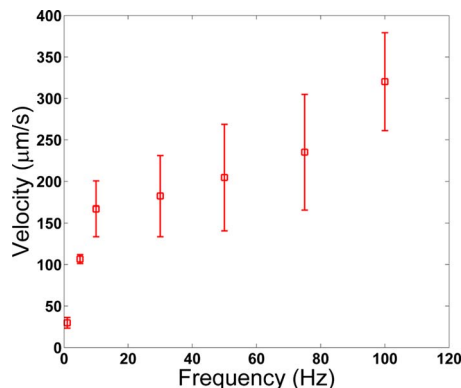


FIG. 2. (Color online) Microtransporter velocity as a function of pulsing frequency. Each data point represents five measurements and error bars indicate one standard error.

from 1% to 10% and fabricated microstructures with different shapes and thickness (30–75 μm). In the application presented in this letter, cells that resemble spheres with a diameter of 50 μm were manipulated. Based on this geometry, we optimized our fabrication procedure for a specific weight ratio (8% by weight) and photoresist thickness (50 μm) and fabricated $100 \times 110 \times 50 \mu\text{m}^3$ U-shaped microtransporters, as shown in Fig. 1(b). The transporters were magnetized in the direction of the opening of the U shape.

Microtransporters were released into the standard medium which we used in cell manipulation experiments to obtain an accurate characterization of their motion. We were able to overcome surface friction, adhesion forces and the drag force acting on the transporters and translate them by applying a static magnetic field exceeding 50 mT using the rectangular NdFeB magnet. However, controlling the motion precisely by adjusting the position of magnets is quite challenging. Instead, as described elsewhere,²⁴ a controllable stick-slip motion is achieved by applying time-varying magnetic fields using electromagnetic coils. Briefly, an in-plane constant field of 5 mT is applied which orients the microtransporters but the force exerted is not high enough to overcome the frictional forces to translate them. A sinusoidal out-of-plane field with amplitude of 1 mT is applied using an electromagnetic coil placed beneath the surface which induces a rocking motion. The magnetic torque tends to align the magnetization of the transporter with the applied fields

$$T = V(\mathbf{M} \times \mathbf{B}), \quad (1)$$

where V and \mathbf{M} is the volume and average magnetization of the microtransporter and \mathbf{B} is the applied magnetic field. The magnetic force exerted on the transporter is proportional to the amplitude of the gradient of the magnetic field according to

$$F = V(\mathbf{M} \cdot \nabla)\mathbf{B}. \quad (2)$$

Several trials were performed by varying the pulsing frequency (1–100 Hz). Imaging was performed on a Leica DMIRB inverted microscope with an automated stage, and videos were captured using a high-speed camera (Redlake Motion Pro X-3). A tracking algorithm was designed to analyze the motion of the geometric centroid. The transporter velocity increases monotonically with frequency, as shown in Fig. 2. A similar trend has been reported elsewhere.²⁴ Depending on the direction of magnetization, different head-to-

tail orientations can be obtained for the same type of structure. When transporters are close to each other, they snap together. Since we can control the magnetization values, the snap-into-contact distance can be adjusted.

As a demonstration of the ability to manipulate single cells, we separated dead *T. pyriformis* cells from living ones using the microtransporters (see supplemental video available online).²⁵ *T. pyriformis* is a protozoan that swims using cilia, a common locomotive appendage in eukaryotes. It is frequently used as a model cell in biochemistry and cell biology due to its complex genetic and structural makeup.²⁶ Cells are cultured using standard medium containing 0.1% yeast extract and 1% tryptone (Difco, Michigan, USA) solved in distilled water.²⁷ The cells were deciliated with a local anesthetic called dibucaine resulting in a suspension of nonmotile cells that do not adhere to the surface.²⁸ Exposing the cells to the anesthetic for 3–5 min is long enough to completely detach cilia without killing them. We extended this period in order to have a heterogeneous population of deciliated dead and live *T. pyriformis* cells. Cultures to be deciliated (cell density 10^5 cells ml^{-1}) were suspended in 1.8 mL of standard medium and 0.2 mL 0.5 mM dibucaine HCl (Sigma-Aldrich, USA). After 6 min of exposure, the cells were transferred to the standard medium. We verified that all cell motility was lost using phase-contrast microscopy.

Cells and microtransporters were released into the same open channel. First, a microtransporter/target pair was selected and the center of mass of the target dead cell was calculated using our tracking algorithm. These cells can easily be detected due to their distinct morphological appearance. They have a spherical shape while live cells look like ellipsoids. Next, the orientation of the transporter was adjusted according to the position of the target cell [Fig. 3(a)]. In the absence of an out-of-plane magnetic field, the transporter was kept in position while the orientation was changed. By applying a time-varying field with a pulsing frequency of 100 Hz, we were able to induce a smooth motion and translate the transporter toward the target cell and accomplish the engagement [Fig. 3(b)]. Finally, the cell was cleared out of the field of view [Fig. 3(c)]. In our experiments, while the manipulation of target cells was performed, the position of other cells kept unchanged unless they were in close proximity (less than 100 μm). This is expected since the flow in the far field falls off inversely with the square of the distance in the low Reynolds regime. We were able to release transported cells and use the same microtransporter multiple times. However, this result cannot be generalized for other cell types.

For applications in which target cells look physically similar to the rest of the cells, fluorescence microscopy can be employed. Target cells can be labeled using fluorescent dyes, fluorescent proteins (i.e., GFP) or quantum dots. To test the feasibility of our tracking algorithm under fluorescent illumination, we acquired images using several excitation/emission filter combinations with a 100 W mercury lamp source. The microtransporters were visible with clear contours which make tracking possible [Fig. 1(c)].

In order to accomplish the manipulation of cells in a fully automated fashion and estimate the forces applied to the cells by the transporters, we are currently developing an experimentally validated mathematical model describing the dynamics of the system. The behavior of the microtransport-

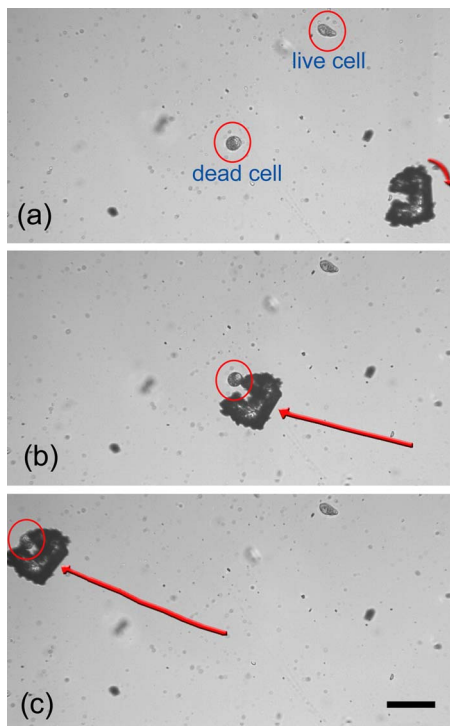


FIG. 3. (Color online) Transport of target cells. (a) The orientation of the transporter is adjusted according to the position of the target cell. (b) With the application of an out-of-plane time-varying magnetic field, the transporter starts translating toward the target. The pulsing frequency is 100 Hz. (c) The target is engaged and transported out of the field of view. The average velocity of the transporter is $350 \mu\text{m/s}$. The scale bar is $100 \mu\text{m}$.

ers depends on their shape, the weight ratio of the suspended magnetite particles, the strength of the applied magnetic fields and the excitation waveform driving the electromagnets. The effect of each factor needs to be characterized to optimize the overall performance. The microfabrication process can also be improved by measuring the optical properties of the ferromagnetic photoresist and accordingly optimizing the exposure time.²⁰

In this letter, a simple method for the fabrication of truly micron-sized, ferromagnetic structures was implemented to fabricate microtransporters. We also demonstrated that single cells can be separated based on their shape without disturbing the local environment. The application area is not limited to cell transport. Positioning cells inside microfluidic channels for single cell analysis is one possibility. We are planning to apply forces locally to specific regions of the cells and examine the cellular reaction to these applied forces.

We would like to thank Dr. Orsolya Láng for her initial contributions in preparing cells and education on working with *T. pyriformis*. We also thank Kivilcim Buyukhatipoglu and Selman Erol for helpful discussions. This work is partially supported by National Science Foundation CAREER Grant No. CMMI-0745019, NSF Grant No. CBET-0828167, and ARO MURI SWARMS Grant No. W911NF.

- ¹J. P. Desai, A. Pillarisetti, and A. D. Brooks, *Annu. Rev. Biomed. Eng.* **9**, 35 (2007).
- ²J. Castillo, M. Dimaki, and W. E. Svendsen, *Integr. Biol.* **1**, 30 (2009).
- ³E. W. H. Jager, O. Inganas, and I. Lundstrom, *Science* **288**, 2335 (2000).
- ⁴R. Dreyfus, M. L. Roper, H. A. Stone, and J. Bibette, *Nature (London)* **437**, 862 (2005).
- ⁵B. R. Donald, C. G. Levey, and I. Paprotny, *J. Microelectromech. Syst.* **17**, 789 (2008).
- ⁶S. T. Chang, V. N. Paunov, D. N. Petsev, and O. D. Velev, *Nature Mater.* **6**, 235 (2007).
- ⁷M. Dauge, M. Gauthier, and E. Piat, *Sens. Actuators, A* **138**, 239 (2007).
- ⁸K. Vollmers, D. R. Frutiger, B. E. Kratochvil, and B. J. Nelson, *Appl. Phys. Lett.* **92**, 144103 (2008).
- ⁹C. Pawashe, S. Floyd, and M. Sitti, *Appl. Phys. Lett.* **94**, 164108 (2009).
- ¹⁰L. Zhang, J. J. Abbott, L. Dong, B. E. Kratochvil, D. Bell, and B. J. Nelson, *Appl. Phys. Lett.* **94**, 064107 (2009).
- ¹¹A. Ghosh and P. Fischer, *Nano Lett.* **9**, 2243 (2009).
- ¹²T. G. Leong, C. L. Randall, B. R. Benson, N. Bassik, G. M. Stern, and D. H. Gracias, *Proc. Natl. Acad. Sci. U.S.A.* **106**, 703 (2009).
- ¹³N. Darnton, L. Turner, K. Breuer, and H. C. Berg, *Biophys. J.* **86**, 1863 (2004).
- ¹⁴D. B. Weibel, P. Garstecki, D. Ryan, W. R. DiLuzio, M. Mayer, J. E. Seto, and G. M. Whitesides, *Proc. Natl. Acad. Sci. U.S.A.* **102**, 11963 (2005).
- ¹⁵Y. Hiratsuka, M. Miyata, T. Tada, and T. Q. P. Uyeda, *Proc. Natl. Acad. Sci. U.S.A.* **103**, 13618 (2006).
- ¹⁶S. Martel, C. C. Tremblay, S. Ngakeng, and G. Langlois, *Appl. Phys. Lett.* **89**, 233904 (2006).
- ¹⁷B. Behkam and M. Sitti, *Appl. Phys. Lett.* **90**, 023902 (2007).
- ¹⁸E. Steager, C.-B. Kim, J. Patel, S. Bith, C. Naik, L. Reber, and M. J. Kim, *Appl. Phys. Lett.* **90**, 263901 (2007).
- ¹⁹M. S. Sakar, E. Steager, A. A. Julius, M. J. Kim, V. Kumar, and G. J. Pappas, Proceedings of IEEE Conference on Robotics and Automation, Anchorage, Alaska, 2010 (unpublished).
- ²⁰N. Damean, B. A. Parviz, J. N. Lee, T. Odom, and G. M. Whitesides, *J. Micromech. Microeng.* **15**, 29 (2005).
- ²¹P. Garstecki, P. Tierno, D. B. Weibel, F. Sagues, and G. M. Whitesides, *J. Phys.: Condens. Matter* **21**, 204110 (2009).
- ²²Y. Yamanishi, S. Sakuma, K. Onda, and F. Arai, *J. Micro-Nano Mech.* **4**, 49 (2008).
- ²³V. Linder, B. D. Gates, D. Ryan, B. A. Parviz, and G. M. Whitesides, *Small* **1**, 730 (2005).
- ²⁴C. Pawashe, S. Floyd, and M. Sitti, *Int. J. Robot. Res.* **28**, 1077 (2009).
- ²⁵See supplementary material at <http://dx.doi.org/10.1063/1.3293457> for video showing the microtransporter manipulating a dead *T. pyriformis* cell.
- ²⁶G. Csaba, *Int. Rev. Cytol.* **95**, 327 (1985).
- ²⁷L. Kohidai and G. Csaba, *Comp. Biochem. Physiol., Part C: Pharmacol., Toxicol. Endocrinol.* **111**, 311 (1995).
- ²⁸G. A. Thompson, L. C. Baugh, and L. F. Walker, *J. Cell Biol.* **61**, 253 (1974).